SCIENCE CHINA
Information Sciences

February 2021, Vol. 64 120302:1–120302:14
https://doi.org/10.1007/s11432-020-2911-0

• RESEARCH PAPER •
Special Focus on Ultra-Reliable Low-Latency Communications in Wireless Networks

Dynamic relay access for D2D-aided low-latency and high-reliability communications

Chun WU[1], Mingming WU[2], Yulan GAO[2], Yue XIAO[2*] & Xiaojian YOU[1]

[1]*School of National Defense Science and Technology, Southwest University of Science and Technology, Mianyang* 621010*, China;*
[2]*National Key Laboratory of Science and Technology on Communications, University of Electronic Science and Technology of China, Chengdu* 611731*, China*

Received 14 January 2020/Accepted 22 April 2020/Published online 14 January 2021

Abstract Device-to-device (D2D) communications allow direct connections among devices to lower transmission latency and network loads of the existing cellular mobile networks. To fully exploit the benefits of D2D communications, relay access is one of the critical challenges upon employing the optimal cooperative relay user equipments (UEs) for data forwarding. The existed relay access approaches usually neglect the inherent motivation that whether the relay is reluctant to forward the information of other UEs based on its status, such as limited battery, service cost and social ties. In this paper, we jointly investigate both the transmission delay and the reliability performance for designing a relay access scheme combined with the impacts of the physical layer and the social layer. Meanwhile, considering the user mobility and status, a dynamic relay access model is constructed with the utility function of the weighted average of latency and social trust level under the long-term constraints. To solve this problem, Lyapunov framework is proposed for converting it into a renewal-reward system towards infinite time horizon, and numerical results show the benefits of the proposed scheme compared with other schemes under dynamic scenarios, as it can lower the latency while guaranteeing the reliability of relay access.

Keywords D2D communications, relay access, low-latency, high-reliability, social ties

Citation Wu C, Wu M M, Gao Y L, et al. Dynamic relay access for D2D-aided low-latency and high-reliability communications. Sci China Inf Sci, 2021, 64(2): 120302, https://doi.org/10.1007/s11432-020-2911-0

1 Introduction

With the 1000-fold capacity increase and ubiquitous wireless connectivity for at least 100 billion devices, the conventional cellular mobile networks are facing with the serious challenges, due to the scarce spectrum, nearly saturated capacity and limited energy of devices [1, 2]. Although densely deploying base stations can improve the transmission rate and the channel capacity partly, such centralized networks are not enough for all the users to achieve the expected performance in real time, owing to the limitations of the processing ability [3, 4]. To deal with the above problems, D2D communications, that enable devices in close proximity to set up the direct connections with each other, have attracted extensive research interests [5–8].

D2D communications can not only support the developments of the distributed networks, such as mobile ad hoc networks (MANET) [9], but also assist in the centralized networks to extend the communication range, offload the data and decrease the transmission delay, such as D2D-aided cellular networks [10]. In addition to the direct communications among devices, another application of D2D communications is the D2D relay, which allows one device to employ other devices as relays to forward its data without the aid of the base station (BS) or other access points [1, 11]. Among the related studies of D2D relay communications, efficient resource management is one of the research focuses, especially for the co-existing scenario of cellular and D2D relay devices where the heterogeneous devices need to share the same resources [12]. Specifically, resource management can be divided into resource allocation and

* Corresponding author (email: xiaoyue@uestc.edu.cn)

relay access or mode selection (single-hop and multi-hop) further [13,14], where resource allocation aims at the interference avoidance and efficient resource utilization, such as power, channel, and bandwidth. For example, a distributed frequency scheduling method was proposed in [15] to maximize the spectral efficiency subject to the channel uncertainties. Energy efficient power allocation for green vehicular networks with cooperative two-hop D2D communications was investigated in [16]. On the other hand, due to the limited number of D2D relays and different demands of source nodes, relay access is another important consideration in resource management for designing reasonable routings to improve the system performance. In [17], relay access and resource allocation were investigated for the network throughput maximization problem by the iterative Hungarian method. Ref. [18] jointly considered several criteria including rate, battery energy, and transmission delay, to maximize the total amount of forwarding data in D2D relay communications.

Moreover, the randomness of channels and the movements of terminals introduce the dynamics for relay selection, where the update of node states and the variation of channel conditions such as location, available power, idle or busy, need to be taken into account for relay handover and update in real time. Related to the dynamic relay selection, some studies have been made to achieve the seamless connections and optimized performance under dynamic mobile networks. Specifically, authors of [19] maximized the sum throughput by optimizing the relay probing time under the delay constraints on each epoch. However, most of the current studies optimize the system objectives under the short-term constraints, which pay more attention to the satisfaction of short-term constraints but ignore the long-term system performance. Owing to the discreteness and finiteness of D2D relays, it is difficult for all the source nodes to select optimal relays that can satisfy the constraints during each frame or at the cost of degraded system performance. Thus, under certain scenarios where users or devices are insensitive to the momentary fluctuations of short-term performance, the long-term constraints may be more proper for the stability and improvement of the system performance [20,21].

Furthermore, as the owner of devices, human behaviours have important effects on the physical transmission from the network topology to the system performance [22–24]. Especially for nowadays, the fast developments of online social networks make a closer relationship between devices and users, which motivates us to integrate the impacts of the social layer into D2D relay communications. Specifically, social ties as the motivation for users to provide relay services could be utilized to construct the network topology combined with the physical connection, and determine whether the user would like to act as relays, based on the social trust level, e.g., the higher social trust level leads to the higher service intention [25,26]. In addition, the participation of the third party in the information interaction increases the security risks for D2D relay communications, such as being eavesdropped, being tampered and information leakage. Thus, it is important for the source nodes to employ trusted relays to guarantee information security and user privacy. Following this line, a lot of researches have been done in terms of the trust management and social trust assessment [27,28]. For example, the quantitative measure model of the social trust level was proposed based on the frequency and duration of contacts in [28]. Ref. [29] investigated the dynamic relay selection problem to achieve the tradeoff between rate and privacy performance based on the social trust level.

Against this background, our main contributions are described as follows.

(1) To lower the latency of edge devices that are far away from the BS and suffer from the terrible channel conditions, certain devices are employed as relays to forward data by D2D relay communications, where the relay selection problem is highlighted for designing appropriate routings. In addition, the impacts of the physical layer and the social layer on relay selection are jointly considered by the weighted average of latency and social ties, where social ties among users are regarded not only as the motivation for relay services, but also the metric of security performance based on the social trust level.

(2) Furthermore, considering the user mobility and channel randomness, we construct a dynamic relay selection model by introducing the definitions of time frame and the long-term constraints, which include the average utility-time ratio of source nodes and the average tolerable satisfaction-time ratio of relays. The Markovian effects among frames imposed by the long-term constraints make the static optimization scheme improper, and thus, the Lyaponov framework and related dynamic algorithm are utilized to convert the dynamic optimization problem into an unconstrained renewal-reward problem towards infinite time horizon.

The rest of this paper is organized as follows. In Section 2, we detail the system model under the D2D-aided cellular networks, including the basic settings of the physical layer and the definitions of the social layer. Section 3 highlights the dynamics of relay selection imposed by the update of node state

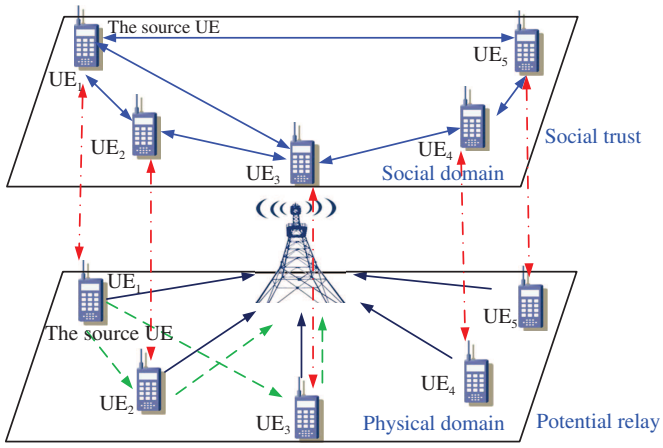

Figure 1 (Color online) System overview for the social-aware cellular mobile network.

and channel conditions, and construct an optimization objective that is the weighted average of delay satisfaction and social trust level under the long-term constraints. In Section 4, the Lyaponov framework is utilized for analyzing the above dynamic optimization problem, and the related algorithm is given for obtaining the optimal relay selection. Section 5 provides numerical results, which demonstrate the effectiveness and benefits of the proposed scheme under the dynamic scenarios. Finally, we conclude in Section 6.

2 System model

Assuming a social-aware cellular mobile network consisting of the physical architecture and the social architecture as depicted in Figure 1, which includes a single BS and several user equipments (UEs) distributed in its coverage, defined as the UEs set $\boldsymbol{U} = \{u_1, u_2, \ldots, u_{N+M}\}$. With the aid of D2D communications, we assume that every UE could be a source node or as a relay to upload other UEs' data to the BS. The source UEs set is denoted as $U_s = \{u_1^s, u_2^s, \ldots, u_N^s\}$ and the potential relays set is denoted as $\mathcal{U} = \{u_1^r, u_2^r, \ldots, u_M^r\}$. For the ease of notation, we consider the single-hop transmission as a special multi-hop routing and the BS as a special relay denoted as u_0^r. Thus, the relay set is extended to $U_r = u_0^r \cup \mathcal{U}$ of $M+1$ relay nodes. To avoid the mutual interferences among UEs, we assume different UEs occupy independent bandwidth W, i.e., frequency division multiple access (FDMA). In addition, relays adopt frequency division duplex (FDD) and decode-and-forward (DF) modes, where the channel bandwidth of two-phase transmission, i.e., source-relay, relay-destination is provided by the source UE and the relay UE, respectively. Thus, if the selected relay has its own tasks to deal with, it has to terminate its tasks or reject the service requirements according to its state and the social ties with the source UE.

2.1 Physical architecture

Likewise, in our mobility model, the UEs can deploy within the coverage circle of the BS, which can be regarded as a renewal system where the system state is refreshed regularly, including the UEs location, available power, and channel conditions. To decrease the heavy signaling overheads imposed by the frequent update of node state information, the passive update mode is adopted in our model, where the relay update is carried out only when the detected rate is lower than the preset threshold. Let $t_0, t_1, t_2, \ldots$ be a sequence of time with the property that $t_{i+1} = t_i + \Delta t, i = 0, 1, 2, \ldots$, where $\Delta t > 0$ is the event-detecting period. At each time of this sequence, the source UE decides whether or not to trigger the selection process based on the received rate. Similar to [21], we define the duration frames as $\{T[0], T[1], \ldots\}$, where $T[i]$ consists of all the slots between the $(i-1)$th and ith relay access switch.

Without loss of generality, we consider a 2D Cartesian coordinate system. Thus, at the beginning of frame r, the coordinate of each UE $u_i \in \boldsymbol{U}$ is $(x_i^{(1)}[r], x_i^{(2)}[r])$. Moreover, since the location of the BS does not change, we assume its location at the origin as any positive integer r, i.e., $(x_0^{(1)}, x_0^{(2)}) = (0, 0)$. For simplifying the illustration we assume that the communication channels are dominated by Log-normal

shadowing model with Rayleigh fading. Therefore, the channel gain from the source UEs u_i^s to any other relay UE $u_j^r \in \mathcal{U}$ as follows:

$$\begin{aligned} &h_{u_i^s,u_j^r}[r] = 10^{-\mathrm{PL}(d)/10}, \\ &\mathrm{PL}(d)[\mathrm{dB}] = \mathrm{PL}_F(d_0) + 10n\log\left(\frac{d[r]}{d_0}\right) + X_\sigma[r], \end{aligned} \tag{1}$$

where n denotes the path-loss exponent, with the reference distance d_0 for D2D links.

Let P_i^s denote the transmission power by source UE u_i^s at the rth frame. The signal noise ratio (SNR) from source UE to the relay can be expressed as

$$\gamma_{u_i^s,u_j^r}[r] = \frac{P_i^s h_{u_i^s,u_j^r}[r]}{n_0^2 W}, \tag{2}$$

where n_0^2 denotes the noise power density.

Accordingly, the achievable rate of the channel is

$$R_{u_i^s,u_j^r}[r] = W\log_2\left(1+\gamma_{u_i^s,u_j^r}[r]\right). \tag{3}$$

In addition, the channel gain from the source UE to the BS directly follows the Log-distance path loss model as

$$\begin{aligned} &h_{u_i^s,u_0^r} = -10^{-\mathrm{PL_{LD}}(d)/10}, \\ &\mathrm{PL_{LD}}(d)[\mathrm{dB}] = \mathrm{PL}_F(d_1) + 10n\log_{10}\left(\frac{d[r]}{d_1}\right), \end{aligned} \tag{4}$$

where d_1 denotes the reference distance for cellular links. The SNR from the source UE to the BS can be expressed as

$$\gamma_{u_i^s,u_0^r}[r] = \frac{P_i^s h_{u_i^s,u_0^r}[r]}{n_0^2 W}, \tag{5}$$

and the corresponding achievable rate is

$$R_{u_i^s,u_0^r}[r] = W\log_2\left(1+\gamma_{u_i^s,u_0^r}[r]\right). \tag{6}$$

The channel gain from the relay UE $u_i^r \in \mathcal{U}$ to the BS is

$$\begin{aligned} &h_{u_j^r,u_0} = -10^{-\mathrm{PL_{LD}}(d)/10}, \\ &\mathrm{PL_{LD}}(d)[\mathrm{dB}] = \mathrm{PL}_F(d_1) + 10n\log_{10}\left(\frac{d[r]}{d_1}\right), \end{aligned} \tag{7}$$

and the corresponding SNR is

$$\gamma_{u_j^r,u_0}[r] = \frac{P_{u_j^r} h_{u_j^r,u_0}[r]}{n_0^2 W}, \tag{8}$$

where $P_{u_j^r}$ represents the transmission power by UE u_j^r at the beginning of frame r, then the cooperative achievable rate is

$$R_{u_j^r,u_0}[r] = W\log_2\left(1+\gamma_{u_j^r,u_0}[r]\right). \tag{9}$$

Therefore, the date rate achieved by the source UE u_i^s is given by

$$R_{u_i^s}[r] = \begin{cases} W\log_2\left(1+\gamma_{u_i^s,u_0}[r]\right), & \text{if } u^r_{\boldsymbol{a}_i[r]} = u_0^r, \\ W\min\left\{\log_2\left(1+\gamma_{u_i^s,u^r_{\boldsymbol{a}_i[r]}}[r]\right), \log_2\left(1+\gamma_{u_i^s,u_0}[r]+\gamma_{u^r_{\boldsymbol{a}_i[r]},u_0}[r]\right)\right\}, & \text{else if } u^r_{\boldsymbol{a}_i[r]} \in \mathcal{U}. \end{cases} \tag{10}$$

Then, the time length of certain frame when the source UE transmits a data package whose size is $Q_i^s[r]$, can be given by

$$T_i[r] = Q_i^s[r]/R_{u_i^s}[r]. \tag{11}$$

2.2 Social architecture

As the rapid development of social networks and smart terminals, the mutual relationships between devices and human have become inseparable gradually, which motivates us to take into account the effects of social ties on D2D relaying. The effectiveness of the relay assistance for cooperative D2D communications is various depending on the knowledge of human social ties. Specifically, social ties as the motivation for users to provide relay services can be utilized to construct the network topology combined with the physical connection. In addition, as mentioned before, social ties can also regarded as the quantitative measure of the security performance to improve the reliability of D2D relay transmission.

Next, we introduce the definition of the social trust level for D2D relay communications. In particular, at the beginning of frame r, a social trust level matrix $\boldsymbol{w}_{N\times(M+1)}[r]$ is introduced varying over time, where the element of matrix ω_{ij} is the social trust degree between two devices u_i^s and u_j^r. A social trust variable ω_{ij} is used to indicate if UEs u_i^s and u_j^r have social trust between each other, as

$$\omega_{ij}=\begin{cases}(0,1], & \text{if } u_i^s \text{ and } u_j^r \text{ have social trust,}\\ 0, & \text{otherwise.}\end{cases} \tag{12}$$

In addition, we assume $\omega_{i0}=1$, $\forall u_i^s\in U_s$, which means that the BS is totally trusted by the source nodes. Therefore, the source UE u_i^s can exploit the trust UEs that have social trust toward it, when $\omega_{ij}>0$, $u_j^r\in U_r$, to improve the reliability of D2D cooperative communications.

Social trust level could be regarded as the quantitative measure of the security performance during the D2D relay transmission, where the multi-hop routing could bring the security risks, such as being eavesdropped, being tampered and information leakage. Moreover, it could also act as the measure of the motivation for the UEs to provide relay service based on the social trust level, e.g., higher social trust level leads to higher service willingness.

3 Dynamic optimization problem formulation

The state space is denoted by $\mathcal{S}$. At each frame r, an element $\boldsymbol{s}[r]\in\mathcal{S}$, and this state consists of $(\boldsymbol{x}_s[r],\boldsymbol{x}_r[r],\boldsymbol{w}[r],\boldsymbol{Q}[r])$, where $\boldsymbol{x}_s[r]=(x_1^s[r],x_2^s[r],\ldots,x_N^s[r])$ is the location of the source UEs, and those of the relays, denoted by $\boldsymbol{x}_r[r]=(x_0^r[r],x_1^r[r],\ldots,x_M^r[r])$ and the transmitted date amount, defined by $\boldsymbol{Q}[r]=(Q_1^s,Q_2^s,\ldots,Q_N^s)$. The source UE accesses a relay from U_r to forward data relying on the current status. The relay selection problem is completely specified by the state space $\mathcal{S}$ and a random function that maps each element $\boldsymbol{s}[r]\in\mathcal{S}$ to a random node $\boldsymbol{a}_{N\times1}[r]\in\mathcal{A}_{\boldsymbol{s}[r]}$, where $\boldsymbol{a}_{N\times1}[r]$ is called an action vector and $\mathcal{A}_{\boldsymbol{s}[r]}\subseteq\tilde{\mathcal{U}}$ is the action space. Let the frame of duration $\boldsymbol{T}[r]=(T_1[r],T_2[r],\ldots,T_N[r])$ denote the time used to transmit the data for the source UEs, at the start of frame r, fixed state $\boldsymbol{s}[r]$ and the action $\boldsymbol{a}[r]$. In addition, the frame of duration $\boldsymbol{T}[r]$ is assumed to have the first and second moments. That is, there are finite constants $\boldsymbol{T}_{N\times1}^{\max}$, $\boldsymbol{T}_{N\times1}^{\min}$, $\boldsymbol{d}_{N\times1}$ such that

$$\begin{aligned}&\boldsymbol{T}^{\min}\leqslant \mathrm{E}\{\boldsymbol{T}[r]\}\leqslant \boldsymbol{T}^{\max},\\ &\mathrm{E}\{\boldsymbol{T}^2[r]\}\leqslant \boldsymbol{d}.\end{aligned} \tag{13}$$

3.1 Utility function

The design of the utility function has critical impacts on the effectiveness of relay selection. To jointly consider both the transmission delay and the reliability performance, we first introduce the mapping function of delay satisfaction to convert the transmission delay into a $[0,1]$ interval. Benefits from the unified value range of delay satisfaction and social trust level, the difference of measurement units can be avoided and the balance between latency and reliability can be achieved better. Inspired by the work in [30], the mapping function of delay satisfaction is defined as

$$f(T)=\begin{cases}1-a\cdot \mathrm{e}^{b\cdot T}, & \text{if } f(T)\geqslant 0,\\ 0, & \text{otherwise,}\end{cases} \tag{14}$$

where a and b are strictly positive real numbers, which can be determined by the practical requirements, e.g., the delay satisfaction needs to approach to 0 when the transmission delay is higher than the preset threshold.

Despite of some similarity with the utility function presented in [29], the defined utility function in the following is different on two aspects: (1) our utility function is more general and reasonable, because the introduced mapping function balances the impacts of different metrics; (2) in our case the social ties and the relay itself state are jointly considered.

Definition 1. The utility function $F_i[r]$ that jointly captures the latency and the reliability performance of the source UE u_i^s is defined as

$$F_i[r] = \beta\omega_{i\boldsymbol{a}_i[r]}[r] + (1-\beta)f(T_{u_i^s}[r]), \tag{15}$$

with $0 \leqslant \beta \leqslant 1$ being the balance coefficient between the latency and the reliability performance for the source UE. Since $\boldsymbol{s}[r]$ is a random variable, the utility function $F_i[r]$ is also random. We assume its first and second moments are bounded by

$$\begin{aligned} &F_i^{\min} \leqslant \mathrm{E}\{F[r]\} \leqslant F_i^{\max}, \\ &\mathrm{E}\left\{F_i^2[r]\right\} \leqslant d_i. \end{aligned} \tag{16}$$

3.2 Problem formulation

To maximize the expectation of the utility function for all the source UEs by selecting the optimal actions, we define the frame-average expectations for all positive integers τ as

$$\bar{F}[r] = \frac{1}{N}\sum_{i=1}^{N}\frac{1}{r}\sum_{\tau=0}^{r-1}\mathrm{E}\{F_i[\tau]\} = \frac{1}{r}\sum_{\tau=0}^{r-1}F[\tau], \tag{17a}$$

$$\bar{T}_i[r] = \frac{1}{r}\sum_{\tau=0}^{r-1}\mathrm{E}\{T_i[\tau]\},\ \forall u_i^s \in U_s, \tag{17b}$$

where $F[\tau] = \frac{1}{N}\sum_{i=1}^{N}\mathrm{E}\{F_i[\tau]\}$ denotes the system average utility function considering all the source UEs each frame.

Here, the utility maximization problem is stated more precisely using $\underline{\lim}_{r\to\infty}$, which does not require the existence of a limit as

$$(\mathbf{P1}):\quad \max \underline{\lim_{r\to\infty}}\ \bar{F}[r] \tag{18a}$$

$$\text{s.t.}\ \ \underline{\lim_{r\to\infty}}\ \frac{\bar{F}_i[r]}{\bar{T}_i[r]} \geqslant F_i^{\mathrm{TH}},\ \forall u_i^s \in U_s, \tag{18b}$$

where F_i^{TH} is the given threshold for the utility-time ratio of the source UE u_i^s.

Constraint (18b) means the expectation of the utility-time ratio above a certain level. As stated before, the optimization problem (18a) and (18b) also assumes that all the potential relay UEs belong to the same organization and the relay UEs have the full willingness to assist the source UE to forward data and pay less attention to the relay UEs' own status such as benefits and costs, which may be improper for the practical scenarios. Therefore, a reasonable metric is required to determine the motivation degree of the potential relay UEs to join in D2D cooperative communications. Based on the satisfaction mapping function and the utility function of the source UEs, we introduce the figure of merit, which involves two aspects related to the physical-social network as the following.

• The preference of the relays. In D2D social networks, if the links are correlated to a high social trust level, the corresponding relays ($u_j^r \in \mathcal{U}$) are more preferable to provide services in the D2D mode. For simplicity, we assume that the patience from the relay to the source UE is a linear increase with the social trust level toward each other, i.e., $\epsilon_{ij}[r] = k \cdot \omega_{ij}[r]$, $k > 0$.

• The tolerable rate satisfaction of the relays. An additional concern that arises in cooperative D2D communications is the tolerable capacity of the relays, as mobile devices are usually busy with their own tasks. Next, we introduce the tolerable rate satisfaction of the relay based on the function form of the delay satisfaction with different parameter setting, which can be used to determine whether the potential relays would cooperate.

Definition 2. The tolerable rate satisfaction $G_j[r]$ of the relay UE u_j^r is defined as

$$G_{\boldsymbol{a}_i[r]}[r] = \epsilon_{i\boldsymbol{a}_i[r]}[r] \cdot f\big(R_{u_i^s}[r]\big) - f\big(R_{u^r_{\boldsymbol{a}_i[r]},u_0}[r]\big), \tag{19}$$

where $\epsilon_{i\boldsymbol{a}_i[r]}$ is the service motivation factor of the relay UE $u^r_{\boldsymbol{a}_i[r]}$, and $f(R_{u^r_{\boldsymbol{a}_i[r]},u_0}[r])$ is the rate satisfaction when the relay deals with its own tasks. It should be noted that when the relay is idle, its rate satisfaction is 0 since the achievable rate is 0, which shows that the idle UEs have more motivations for providing relay services compared to the busy UEs.

Note that, by using $G_{\boldsymbol{a}_i[r]}[r]$, which represents the total tolerable capacity, the potential relays can make a decision if UE $u^r_{\boldsymbol{a}[r]}$ will act as the relay for the source UE. Similar to the utility function $F_i[r]$, the tolerable rate satisfaction $G_j[r]$ is assumed to have second moments. That is, there is a finite constant d_j such that

$$\mathrm{E}\{G_j^2[r]\} \leqslant d_j. \tag{20}$$

Similarly, we define the frame-average expectations for all positive integers r as

$$\bar{G_j}[r] = \frac{1}{r}\sum_{\tau=0}^{r-1} \mathrm{E}\{G_j[\tau]\}. \tag{21}$$

Likewise, the utility maximization problem is given by

$$(\mathbf{P2}): \quad \max \varliminf_{r\to\infty} \bar{F}[r] \tag{22a}$$

$$\text{s.t.} \quad \varliminf_{r\to\infty} \frac{\bar{F}_i[r]}{\bar{T}_i[r]} \geqslant F_i^{\mathrm{TH}}, \ \forall u_i^s \in U_s, \tag{22b}$$

$$\varliminf_{r\to\infty} \frac{\bar{G}_j[r]}{\bar{T}_i[r]} \geqslant G_j^{\mathrm{TH}}, \ \forall u_j^r \in \mathcal{U}, \tag{22c}$$

where G_j^{TH} is the given threshold for the tolerable rate satisfaction-time ratio. In (22), in each frame r, the optimal strategies $\boldsymbol{a}[r] \in \mathcal{A}_{\boldsymbol{s}[r]}$ can be obtained for maximizing $\bar{F}[r]$. Moreover, (22c) indicates that, the relay allows its device to act as relay for the source UE only when the long-term benefits of the tolerable rate satisfaction exceeds a certain level.

4 Relay selection via Lyapunov framework

Using $\overline{\lim}_{r\to\infty}$, (**P1**) yields to be

$$(\mathbf{P1.1}): \quad \min \overline{\lim_{r\to\infty}} -\bar{F}[r] \tag{23a}$$

$$\text{s.t.} \quad \overline{\lim_{r\to\infty}} -\frac{\bar{F}_i[r]}{\bar{T}_i[r]} \leqslant -F_i^{\mathrm{TH}}. \tag{23b}$$

To satisfy the long-term constraint (23b) while maximizing the time-average utility value, virtual queues $\gamma_i[r]$ are introduced for the corresponding long-term constraint $\frac{\bar{F}_i[r]}{\bar{T}_i[r]}$, and their update expressions are given by

$$\gamma_i[r+1] = \begin{cases} \max\big\{\gamma_i[r] + \big(-F_i[r] + F_i^{\mathrm{TH}}T_i[r]\big), 0\big\}, & r > 0, \\ 0, & r = 0, \end{cases} \tag{24}$$

where

$$F_i^{\mathrm{TH}} = \begin{cases} 0, & u^r_{\boldsymbol{a}_i[r]} = u_0^r, \\ F_i^{\mathrm{TH}}, & \text{otherwise}. \end{cases} \tag{25}$$

Based on the quadratic form $L[r] = \frac{1}{2}\sum_{i=1}^N \gamma_i^2[r]$, the drift of Lyapunov function $\triangle L[r] = L[r+1] - L[r]$ is given by

$$\triangle L[r] = \frac{1}{2}\sum_{i=1}^N \big(F_i^2[r] + 2F_i^{\mathrm{TH}}F_i[r]T_i[r] + (F_i^{\mathrm{TH}})^2T_i^2[r]\big) + \sum_{i=1}^N \gamma_i[r]\big(-F_i[r] + F_i^{\mathrm{TH}}T_i[r]\big). \tag{26}$$

For any possible $\Gamma[r]=[\gamma_1[r],\ldots,\gamma_N[r]]$, taking condition expectations, the one-frame drift $\triangle L[r]$ is bounded by

$$\mathrm{E}\left\{\triangle L_i[r]\right\}\leqslant\underbrace{\frac{1}{2}\sum_{i=1}^{N}\left\{d_i\big(1+2F_i^{\mathrm{TH}}+(F_i^{\mathrm{TH}})^2\big)\right\}}_{\mathcal{B}}+\mathrm{E}\left\{\sum_{i=1}^{N}\gamma_i[r]\big(-F_i[r]+F_i^{\mathrm{TH}}T_i[r]\big)|\Gamma[r]\right\},\tag{27}$$

where B is the constant that satisfies for all r and all possible $\Gamma[r]$.

Furthermore, by employing Lyapunov optimization framework, the constrained problem of (**P1.1**) can be converted into an unconstrained penalty function problem, given by

$$(\mathbf{P1.2}):\ \ \min -VF[r]+\sum_{i=1}^{N}\gamma_i[r]\big(-F_i[r]+F_i^{\mathrm{TH}}T_i[r]\big).\tag{28}$$

The corresponding relay selection algorithm is summarized in Algorithm 1.

Algorithm 1 Relay access algorithm of (**P1**): $\forall r\in N_+$.

Require: Initialize $\boldsymbol{s}[r]$, $\Gamma[r]$, V and F_i^{TH}, G_i^{TH}.
Output: $\boldsymbol{a}[r]$.
1: Compute $F_i[r]$, $T_i[r]$, $\forall i\in\{0,1,2,\ldots,N\}$, respectively;
2: Update the virtual queue $\Gamma[r+1]$ with Eqs. (24) and (25);
3: Find the optimal action in $\mathcal{A}_{s[r]}$ for the optimization problem in Eq. (28).

In order to solve the optimization problem (**P1.2**) by the DPP algorithm, we respectively introduce two virtual queues $\gamma_i^{(1)}[r]$ and $\gamma_j^{(2)}[r]$ as

$$\gamma_j^{(2)}[r+1]=\begin{cases}\max\left\{\gamma_j^{(2)}[r]+\big(-G_j[r]+G_j^{\mathrm{TH}}T_i[r]\big),0\right\}, & r>0,\\ 0, & r=0,\end{cases}\tag{29}$$

where the virtual queue $\gamma_j^{(2)}[r]$ for each relay UE $u_j^r\in\mathcal{U}$ can ensure the quality constraint in (22c), with $\gamma_i^{(1)}[r]=\gamma_i[r]$, $\forall u_i^s\in U_s$. Moreover, we have

$$G_j^{\mathrm{TH}}=\begin{cases}0, & u_j^r=u_0^r,\\ G_j^{\mathrm{TH}}, & u_j^r\in\mathcal{U},\end{cases}\tag{30}$$

and

$$\begin{aligned}\Gamma^{(1)}[r]:=&(\gamma_1^{(1)}[r],\ldots,\gamma_N^{(1)[r]})^{\mathrm{T}},\\ \Gamma^{(2)}[r]:=&(\gamma_1^{(2)}[r],\ldots,\gamma_M^{(2)[r]})^{\mathrm{T}}.\end{aligned}\tag{31}$$

Similar to the analysis of (**P1.1**), with C-additive approximation of action strategy instead of the exact infimum of the objective in (**P2**) and the assumptions of fix constants $\mathcal{C}\geqslant 0$, $\mathcal{V}\geqslant 0$, and for any frame r and any possible $\Upsilon[r]$, (**P2**) is simplified as

$$(\mathbf{P2.1}):\quad \min -\mathcal{V}F[r]+\sum_{n=1}^{M+N}\upsilon_n[r]\left[-p_n[r]+c_n\tilde{T}_n[r]\right],\tag{32}$$

where

$$p_n[r]=\begin{cases}F_n[r], & 1\leqslant n\leqslant N,\\ G_{M+N+1-n}[r], & N+1\leqslant n\leqslant M+N;\end{cases}\tag{33a}$$

$$\tilde{T}_n[r]=\begin{cases}T_n[r], & 1\leqslant n\leqslant N,\\ T_{M+N+1-n}[r], & N+1\leqslant n\leqslant M+N;\end{cases}\tag{33b}$$

$$c_n = \begin{cases} F_n^{\mathrm{TH}}, & 1 \leqslant n \leqslant N, \\ G_{M+N+1-n}^{\mathrm{TH}}, & N+1 \leqslant n \leqslant M+N. \end{cases} \tag{33c}$$

Next, the dynamic relay selection algorithm for (**P2**) is summarized in Algorithm 2, and the following lemma shows its validity, and more details of the proof refer to [21].

Algorithm 2 Relay access algorithm for (**P2**): $\forall r \in N_+$.

Require: Initialize $\boldsymbol{s}[r]$, $\Upsilon[r]$, V and F_{TH}, G_{TH}.
Output: $\boldsymbol{a}[r]$.
1: Compute $F[r]$, $p_i[r]$, $\forall i \in \{1, 2, \ldots, 2N\}$ with Eqs. (15) and (33a), respectively.
2: Update the virtual queue $\Upsilon[r+1]$ with Eqs. (24) and (29).
3: Find the optimal action in $\mathcal{A}_{s[r]}$ for the optimization problem in Eq. (32).

Lemma 1. Assume the constraints of problem (22a)–(22c) are feasible. Fix constants $\mathcal{C} \geqslant 0$, $\mathcal{V} \geqslant 0$, and assume Algorithm 2 is implemented using any C-additive approximation on every frame r for the minimization of (32). Then, for all integers $\tau > 0$ we have

$$\lim_{r\to\infty} \sup -\bar{F}[r] \leqslant -F^{\mathrm{opt}} + \frac{\mathcal{B}+\mathcal{C}}{\mathcal{V}}, \tag{34}$$

where $-F^{\mathrm{opt}}$ is the optimal solution to (22a)–(22c).

5 Numerical simulation

In this section, we evaluate the performance of the proposed relay access scheme jointly considering latency and reliability through extensive numerical simulations. The convergence and effectiveness of the proposed scheme are verified. For our simulations, we consider a circular cell with a radius of 500 m and assume the single BS is placed in the center of the cell. In the cell, there exists several dynamically moving cellular users and D2D pair devices. Since the relay selection is mainly for cellular users far away from the central BS, without loss of generality, we only focus on these cellular users located in the range of $[350, 500]$ m away from the BS while setting the D2D pair moving in the distance of $[100, 300]$ m from the BS. Furthermore, the communication range of the D2D pair device is limited to $[40, 150]$ m. To simplify the analysis, each cellular user is assumed to have the same average utility-time ratio $\bar{F}/\bar{T}$ constraint and each D2D transmitter has the same $\bar{G}/\bar{T}$ constraint. Note that the proposed scheme is also applicable to more complicated scenarios where different cellular users and D2D pairs have various $\bar{F}/\bar{T}$, $\bar{G}/\bar{T}$ constraints.

5.1 Simulation environment and setting

To ensure the reliability of the simulation results, the construction of social-layer network uses real measured data from Inform 06 collected by Cambridge Haggle project [31], which denotes the normalized average contact rate among users as the social trust level. The dynamic mobility process of cellular users and D2D pairs is modeled by the Gauss-Markov mobility model (GMMM), which is widely utilized for the personal mobile telecommunication system (PMC). The details of GMMM are given by

$$\begin{cases} v_t = \delta v_{t-1} + (1-\delta)\bar{v} + (1-\delta^2)\tilde{v}_t, \\ \eta_t = \delta \eta_{t-1} + (1-\delta)\bar{\eta} + (1-\delta^2)\tilde{\eta}_t, \end{cases} \tag{35}$$

where $0 \leqslant \delta \leqslant 1$ is the tuning parameter to regulate the randomness; v_{t-1}, η_{t-1} are the velocity and direction of the previous moment and $\bar{v}$, $\bar{\eta}$ represent the mean value of the velocity and the direction keeping constant for a long time; $\tilde{v}_t$, $\tilde{\eta}_t$ are random variables obeying normalized Gaussian distribution in order to simulate the randomness of mobility. Meanwhile, the updated position is given by

$$\begin{cases} x_t^{(1)} = x_{t-1}^{(1)} + v_{t-1}\cos(\eta_{t-1}), \\ x_t^{(2)} = x_{t-1}^{(2)} + v_{t-1}\sin(\eta_{t-1}). \end{cases} \tag{36}$$

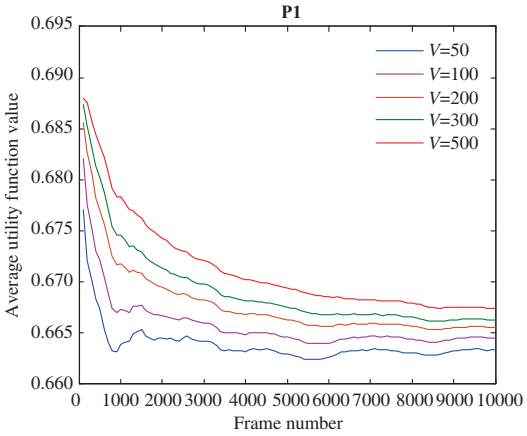

Figure 2 (Color online) The convergence of average utility function value of **P1** versus frame number under different V.

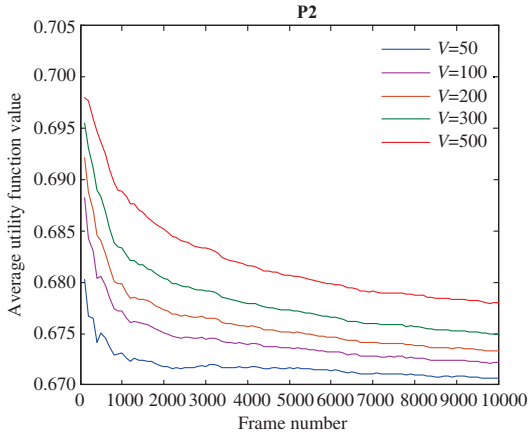

Figure 3 (Color online) The convergence of average utility function value of **P2** versus frame number under different V.

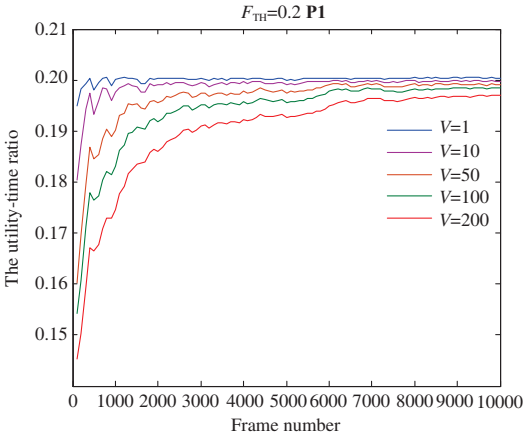

Figure 4 (Color online) The convergence of the first constraint $\bar{F}/\bar{T}$ of **P1** versus frame number under different V.

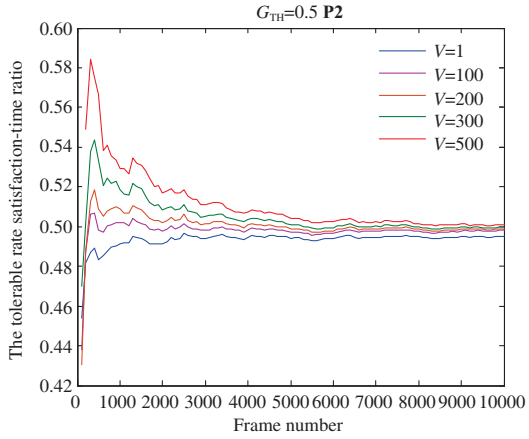

Figure 5 (Color online) The convergence of the second constraint $\bar{G}/\bar{T}$ of **P2** versus frame number under different V.

Specially, we define the BS as the origin of rectangular coordinates. $x_{t-1}^{(1)}$, $x_{t-1}^{(2)}$ are the coordinates of the previous moment. The initial locations of cellular users and D2D pairs are uniformly distributed within the given range. Moreover, the data arrival process is Possion process with an arrival rate λ. The remaining simulation parameters are the same as presented in [21].

5.2 Performance of dynamic relay access algorithm

To verify the convergence of the proposed algorithm and impacts of the adjustable parameter V on the convergence speed, we investigate $\bar{F}/\bar{T}$, $\bar{G}/\bar{T}$ versus frame number with different V value. The results are shown as follows.

Figures 2 and 3 show that the utility function values of **P1**, **P2** gradually decrease as the frame number increases and the lower V leads to the faster convergence speed. It can be explained by that the lower V makes the impact of long-term constraints on the objective function greater in Eqs. (28) and (32), prompting constraints to be satisfied more quickly, which can be observed in Figures 4 and 5 clearly.

In Figure 5, when V is large, $\bar{G}/\bar{T}$ firstly increases beyond the constraint threshold and then falls to the constraint threshold, which is attributed to the coupling relationship between $\bar{G}/\bar{T}$ and the objective function to some extent. By selecting the proper $V/\alpha_1, V/\alpha_2$, the proposed algorithm can converge faster.

In order to assess the influence of the constraint threshold on the performance of the proposed scheme, with fixed β value, different constraint thresholds Y_{TH}, G_{TH} are selected to show their impact on various parameters of the model. Figure 6 describes the utility function value of **P1** and **P2** versus G_{TH} attached to different Y_{TH}, whose left ordinate is for **P1** and right ordinate is for **P2**. In Figure 6, we observe that

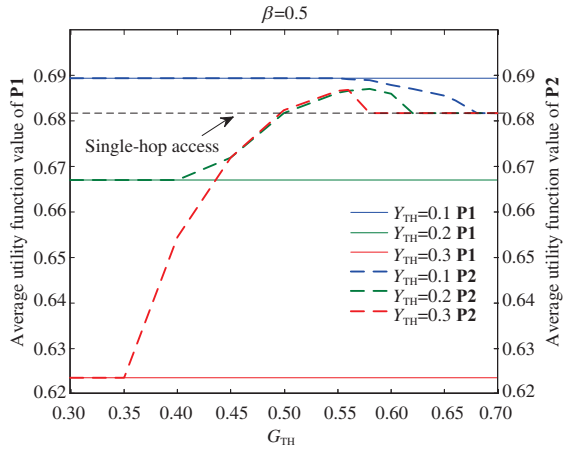

Figure 6 (Color online) The utility function value of **P1**, **P2** versus G_{TH} attached to different Y_{TH}.

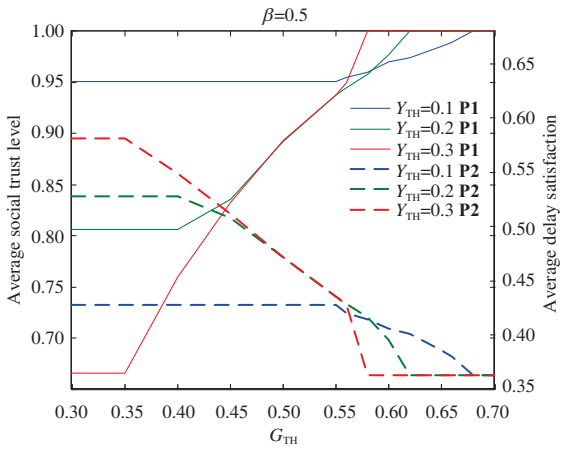

Figure 7 (Color online) The average delay satisfaction and social trust level of **P1**, **P2** versus G_{TH} attached to different Y_{TH}.

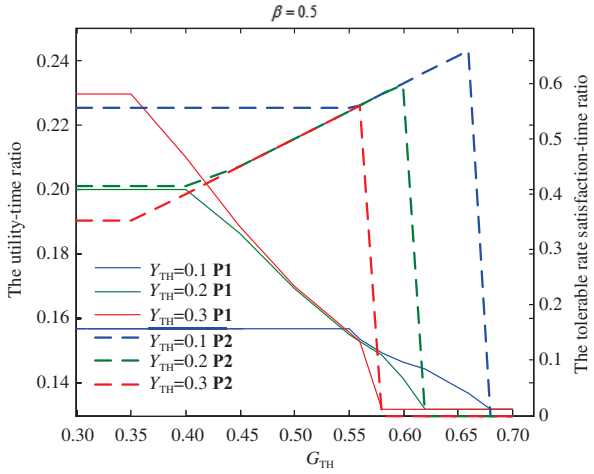

Figure 8 (Color online) The constraint $\bar{F}/\bar{T}$, $\bar{G}/\bar{T}$ of **P1**, **P2** versus G_{TH} attached to different Y_{TH}.

the utility function value of **P1** keeps unchanged when G_{TH} varies, since **P1** has not the second constraint. In addition, higher Y_{TH} values result in lower utility function values of **P1**, since the improvement of the constraint threshold Y_{TH} requires lower average frame length, resulting in a higher average rate requirement, which increases the proportion of delay satisfaction in the objective function, eventually leading to a drop in the utility function value. For **P2** in Figure 6, when G_{TH} is below a certain threshold $G_{\mathrm{TH}}^{\min}$, the constraint does not work, the utility function value remains constant and coincides with the **P1**. Additionally, higher Y_{TH} corresponds to lower $G_{\mathrm{TH}}^{\min}$ required for the second constraint to work, because higher Y_{TH} causes the importance of the social trust level in the utility function to decrease, bringing about the earlier effectiveness of the second constraint. When G_{TH} exceeds $G_{\mathrm{TH}}^{\min}$, it can be observed from Figure 7 that with the increase of G_{TH}, the average social trust level exhibits an upward trend, and the average user satisfaction shows a downward trend. When G_{TH} is greater than a certain threshold $G_{\mathrm{TH}}^{\max}$, the curves attached to different Y_{TH} overlap to the same constant value, and higher Y_{TH} corresponds to lower $G_{\mathrm{TH}}^{\max}$. Also, different curves have various dynamic ranges of $[G_{\mathrm{TH}}^{\min}, G_{\mathrm{TH}}^{\max}]$.

The change of social trust level and delay satisfaction in Figure 7 explains the trend of each curve in Figure 6 with G_{TH} in the range of $[G_{\mathrm{TH}}^{\min}, G_{\mathrm{TH}}^{\max}]$. When G_{TH} is greater than $G_{\mathrm{TH}}^{\max}$, the stricter second constraint forces the cellular user only to select the base station directly, the utility function value eventually coincides with the value of SH. It should be noted that, as G_{TH} has a dynamic ranges $[G_{\mathrm{TH}}^{\min}, G_{\mathrm{TH}}^{\max}]$, where the second constraint makes a difference in the performance of the proposed algorithm, Y_{TH} has also a dynamic range $[Y_{\mathrm{TH}}^{\min}, Y_{\mathrm{TH}}^{\max}]$. Here we just select several typical value to reflect the effect of Y_{TH}, including $Y_{\mathrm{TH}} = 0.1 < Y_{\mathrm{TH}}^{\min}$, $Y_{\mathrm{TH}} = 0.2 \in [Y_{\mathrm{TH}}^{\min}, Y_{\mathrm{TH}}^{\max}]$, $Y_{\mathrm{TH}} = 0.3 > Y_{\mathrm{TH}}^{\max}$. Besides, since the pa-

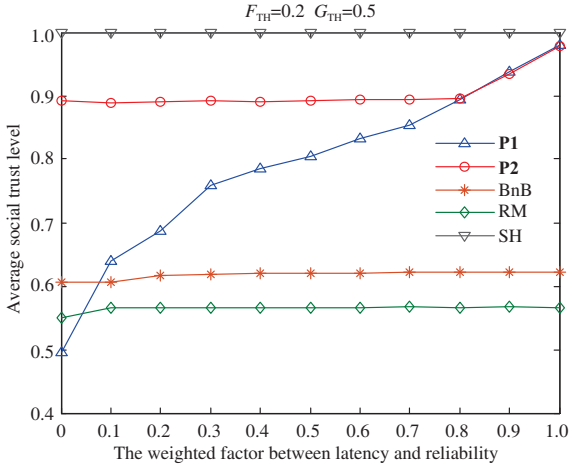

Figure 9 (Color online) The average delay satisfaction degree versus β for different relay access schemes.

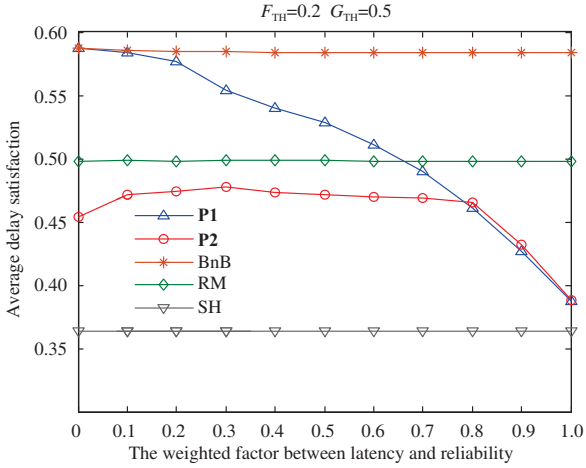

Figure 10 (Color online) The average social trust level versus β for different relay access schemes.

rameters of the **P1** problem do not change with $G_{\rm TH}$, the **P1** problem is equivalent to the **P2** problem when $G_{\rm TH} < G_{\rm TH}^{\min}$. Therefore, to simplify the simulation figure, we will not draw the curves related to parameters of the **P1** problem in Figures 7 and 8, its parameters can refer to the parameters of the **P2** problem when $G_{\rm TH} < G_{\rm TH}^{\min}$.

Figure 8 shows the relationship between $\bar{F}/\bar{T}$ and $\bar{G}/\bar{T}$ attached to different $Y_{\rm TH}$ and $G_{\rm TH}$. It can be seen that under the condition of $G_{\rm TH} < G_{\rm TH}^{\min}$, with the increase of the constraint threshold $Y_{\rm TH}$ from $< Y_{\rm TH}^{\min}$, $[Y_{\rm TH}^{\min}, Y_{\rm TH}^{\max}]$ to $> Y_{\rm TH}^{\max}$, the utility-time ratio $\bar{F}/\bar{T}$ shows the corresponding variation from $Y_{\rm TH}^{\min}$, $Y_{\rm TH}$ to $Y_{\rm TH}^{\max}$. Under the condition of $G_{\rm TH} \in [G_{\rm TH}^{\min}, G_{\rm TH}^{\max}]$, $\bar{F}/\bar{T}$ decreases as $G_{\rm TH}$ increases, due to the fact that the impact of the second constraint on (32) strengthen with $G_{\rm TH}$ increasing, inversely causing the impact of the first constraint weakened; under the condition of $G_{\rm TH} > G_{\rm TH}^{\max}$, all the curves with different $Y_{\rm TH}$ will select the BS for direct transmission, resulting in $\bar{F}/\bar{T}$ values of different curves overlap to a constant value as the single-hop access scheme. Similar to the trend of $\bar{F}/\bar{T}$ versus $G_{\rm TH}$, the trend of $\bar{G}/\bar{T}$ is also divided into three phases: when $G_{\rm TH} < G_{\rm TH}^{\min}$, $\bar{G}/\bar{T} = G_{\rm TH}^{\min}$; when $G_{\rm TH} \in [G_{\rm TH}^{\min}, G_{\rm TH}^{\max}]$, $\bar{G}/\bar{T} = G_{\rm TH}$; when $G_{\rm TH} > G_{\rm TH}^{\max}$, curves all choose the BS to transmit directly, $\bar{G}/\bar{T}$ is undefined and set to zero.

5.3 Performance comparison

To verify the benefits of the proposed scheme, performance comparison is carried out with other relay access schemes, which include the random access (RM), single-hop access (SH) and frame-by-frame static optimization based on the branch-and-bound (BnB) algorithm. It is noted that BnB cannot deal with the dynamic optimization problem towards infinite time horizon, and thus, the constraints of BnB is replaced by the short-term constraints of each frame.

Figures 9 and 10 show the trends of average social trust level and average delay satisfaction versus β. It can be seen from Figure 9 that when β is very small, the average social trust of **P1** approaches the performance of BnB. As β increases, the impact of the social trust level on the utility function improves, thus, the average social trust level of **P1** also gradually increases. Finally, when $\beta = 1$, the average social trust level of **P1** reaches to 1, which is equal to the performance of SH. Different from **P1**, the average social trust level of **P2** is nearly a constant when β is small ($\beta \leqslant 0.8$). The reason is that when β is small, the degree of coupling of the utility function with the second constraint is small, and the constraint of $G_{\rm TH} = 0.5$ is strict, so that **P2** considers the second constraint more compared to the maximization of the utility function. These two factors make the utility function have little effect on the relay selection when $\beta \leqslant 0.8$. When $\beta > 0.8$, the proportion of social trust level in the utility function continues to increase, so that the coupling degree between the utility function and the second constraint becomes sufficiently high, as a result, the second constraint gradually becomes invalid and redundant, the average social trust level curves of **P1** and **P2** are gradually close to each other. Besides, the average social trust level of BnB is stable at around 0.6, and the average social trust level of RM is stable at around 0.55.

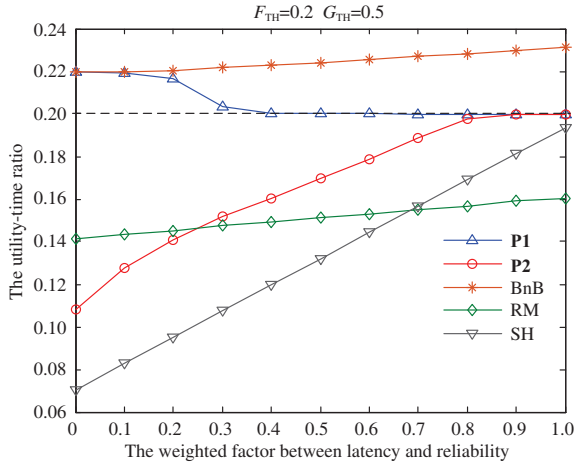

Figure 11 (Color online) The first constraint $\bar{F}/\bar{T}$ versus β for different relay access schemes.

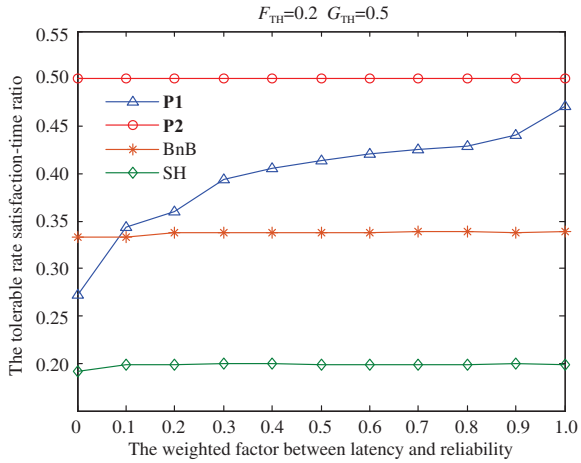

Figure 12 (Color online) The first constraint $\bar{G}/\bar{T}$ versus β for different relay access schemes.

In Figure 10, when β is very small, the average delay satisfaction of **P1** is close to the value of BnB and with the increase of β, the average delay satisfaction of **P1** gradually decreases. On the other hand, **P2** maintains a stable value (0.45 0.46) when $\beta \leqslant 0.8$. When $\beta > 0.8$, the curve of **P2** gradually coincides with the **P1** curve, and the final average delay satisfaction of **P2** is close to the values of SH. In addition, the average delay satisfaction of BnB is around 0.58, the average delay satisfaction of RM is around 0.5, and the average delay satisfaction of SH is only about 0.36.

Figures 11 and 12 show the trends of $\bar{F}/\bar{T}$, $\bar{G}/\bar{T}$. In Figure 11, we observe that when β is small as $\beta \leqslant 0.4$, $\bar{F}/\bar{T}$ of **P1** will be higher than the set threshold, which is attributed to that lower β leads to higher proportion of the delay satisfaction in the utility function, furthermore, resulting in a higher degree of coupling between the first constraint and the utility function, eventually giving rise to the first constraint becomes invalid and redundant. As β continues to increase, the degree of coupling of the utility function with the first constraint is weakened, the first constraint begins to work, in consequence, the $\bar{F}/\bar{T}$ of **P1** is constant near the set threshold $F_{\text{th}} = 0.2$. According to Figures 9 and 10, when $\beta \leqslant 0.8$, the average social trust level and average delay satisfaction of **P2** are basically constant, which explains the reason that the $\bar{F}/\bar{T}$ of **P2** increases with higher β in Figure 11 is just caused by the change of the ratio between two constant values shown in Figures 9 and 10. Similar to **P2**, the $\bar{F}/\bar{T}$ of SH increases linearly with the increase of β, owing to the above reasons also. When $\beta > 0.8$, the second constraint fails, $\bar{F}/\bar{T}$ of **P2** gradually trends towards $\bar{F}/\bar{T}$ of **P1**. $\bar{F}/\bar{T}$ of BnB remains around 0.23. $\bar{F}/\bar{T}$ of RM remains around 0.15. Figure 12 shows that $\bar{G}/\bar{T}$ of **P1** increases gradually with β increasing, because the increase of β leads to an increase in the coupling degree between the utility function and the second constraint, so that $\bar{G}/\bar{T}$ of **P1** without the second constraint also increases gradually, eventually close to $\bar{G}/\bar{T}$ of **P2**. Moreover, $\bar{G}/\bar{T}$ of **P2** could be maintained at the set threshold $G_{\text{TH}} = 0.5$. $\bar{G}/\bar{T}$ of BnB is around 0.34, $\bar{G}/\bar{T}$ of RM is around 0.2.

6 Conclusion

In this paper, we proposed a relay selection scheme under the D2D-aided cellular mobile networks, combined with the impacts of the physical layer and the social layer. The tradeoff between the latency and reliability performance was considered in the system objective with the weighted average of both. Furthermore, a dynamic relay selection problem was analyzed and investigated under the Lyaponov framework. Numerical results show the effects of the proposed scheme, which can lower the transmission delay while guaranteeing the reliability performance of D2D relay communications under the dynamic scenarios.

Acknowledgements This work was supported by National Natural Science Foundation of China (Grant No. 61771410) and National Key R&D Program of China (Grant No. 2018YFC0807101).

References

1 Yang P, Xiao Y, Xiao M, et al. 6G wireless communications: vision and potential techniques. IEEE Netw, 2019, 33: 70–75
2 Andrews J G, Buzzi S, Choi W, et al. What will 5G be? IEEE J Sel Areas Commun, 2014, 32: 1065–1082
3 Boccardi F, Heath R W, Lozano A, et al. Five disruptive technology directions for 5G. IEEE Commun Mag, 2014, 52: 74–80
4 Kamel M, Hamouda W, Youssef A. Ultra-dense networks: a survey. IEEE Commun Surv Tutor, 2016, 18: 2522–2545
5 Tehrani M N, Uysal M, Yanikomeroglu H. Device-to-device communication in 5G cellular networks: challenges, solutions, and future directions. IEEE Commun Mag, 2014, 52: 86–92
6 Bello O, Zeadally S. Intelligent device-to-device communication in the Internet of things. IEEE Syst J, 2016, 10: 1172–1182
7 Jameel F, Hamid Z, Jabeen F, et al. A survey of device-to-device communications: research issues and challenges. IEEE Commun Surv Tutor, 2018, 20: 2133–2168
8 Ansari R I, Chrysostomou C, Hassan S A, et al. 5G D2D networks: techniques, challenges, and future prospects. IEEE Syst J, 2018, 12: 3970–3984
9 Conti M, Giordano S. Mobile ad hoc networking: milestones, challenges, and new research directions. IEEE Commun Mag, 2014, 52: 85–96
10 Feng D Q, Lu L, Yi Y W, et al. Device-to-device communications underlaying cellular networks. IEEE Trans Commun, 2013, 61: 3541–3551
11 Nishiyama H, Ito M, Kato N. Relay-by-smartphone: realizing multihop device-to-device communications. IEEE Commun Mag, 2014, 52: 56–65
12 Yu C H, Doppler K, Ribeiro C B, et al. Resource sharing optimization for device-to-device communication underlaying cellular networks. IEEE Trans Wirel Commun, 2011, 10: 2752–2763
13 Ma R F, Xia N, Chen H H, et al. Mode selection, radio resource allocation, and power coordination in D2D communications. IEEE Wirel Commun, 2017, 24: 112–121
14 Hoang T D, Le L B, Le-Ngoc T. Joint mode selection and resource allocation for relay-based D2D communications. IEEE Commun Lett, 2017, 21: 398–401
15 Hasan M, Hossain E, Kim D I. Resource allocation under channel uncertainties for relay-aided device-to-device communication underlaying LTE-a cellular networks. IEEE Trans Wirel Commun, 2014, 13: 2322–2338
16 Zhou Z Y, Xiong F, Xu C, et al. Energy-efficient vehicular heterogeneous networks for green cities. IEEE Trans Ind Inf, 2018, 14: 1522–1531
17 Kim T, Dong M M. An iterative hungarian method to joint relay selection and resource allocation for D2D communications. IEEE Wirel Commun Lett, 2014, 3: 625–628
18 Ma R, Chang Y J, Chen H H, et al. On relay selection schemes for relay-assisted D2D communications in LTE-A systems. IEEE Trans Veh Technol, 2017, 66: 8303–8314
19 Zhang H, Wang Z H, Du Q H. Social-aware D2D relay networks for stability enhancement: an optimal stopping approach. IEEE Trans Veh Technol, 2018, 67: 8860–8874
20 Neely M J. Dynamic optimization and learning for renewal systems. IEEE Trans Autom Control, 2013, 58: 32–46
21 Gao Y L, Xiao Y, Wu M M, et al. Dynamic social-aware peer selection for cooperative relay management with D2D communications. IEEE Trans Commun, 2019, 67: 3124–3139
22 Lu J, Yao J E, Yu C S. Personal innovativeness, social influences and adoption of wireless Internet services via mobile technology. J Strategic Inf Syst, 2005, 14: 245–268
23 Rahim A, Kong X J, Xia F, et al. Vehicular social networks: a survey. Pervas Mobile Comput, 2018, 43: 96–113
24 Du Q H, Song H B, Zhu X J. Social-feature enabled communications among devices toward the smart IoT community. IEEE Commun Mag, 2019, 57: 130–137
25 Chen X, Proulx B, Gong X W, et al. Exploiting social ties for cooperative D2D communications: a mobile social networking case. IEEE/ACM Trans Netw, 2015, 23: 1471–1484
26 Zhang Z F, Zhang P R, Liu D, et al. SRSM-based adaptive relay selection for D2D communications. IEEE Int Things J, 2018, 5: 2323–2332
27 Cho J H, Swami A, Chen I R. A survey on trust management for mobile ad hoc networks. IEEE Commun Surv Tutor, 2011, 13: 562–583
28 Sherchan W, Nepal S, Paris C. A survey of trust in social networks. ACM Comput Surv, 2013, 45: 1–33
29 Meng Y, Jiang C X, La Q D, et al. Dynamic social-aware peer selection scheme for cooperative device-to-device communications. In: Proceedings of IEEE Wireless Communications and Networking Conference (WCNC), 2017
30 Fiedler M, Hossfeld T, Tran-Gia P. A generic quantitative relationship between quality of experience and quality of service. IEEE Netw, 2010, 24: 36–41
31 Scott J, Gass R, Crowcroft J, et al. Crawdad Dataset Cambridge/Haggle (v. 2006-09-15). Technical Report. 2006